Microwave-assisted Synthesis of 2-(2-Pyridyl)azoles. Study of their Corrosion Inhibiting Properties

Natalya V. Likhanova,[A] M. Aurora Veloz,[B] Herbert Höpfl,[C] Diana J. Matías,[B] Victor E. Reyes-Cruz,[B] Octavio Olivares,[D] and Rafael Martínez-Palou[A,*]

[A] Instituto Mexicano del Petróleo, Eje Central Lázaro Cárdenas No. 152, 07730 México, D.F., México. E-mail: rpalou@imp.mx

[B] Universidad Autónoma del Estado de Hidalgo, Instituto de Ciencias Básicas e Ingeniería, Área de Materiales y Metalurgia, Carr. Pachuca-Tulancingo KM 4.5, 42184, Pachuca, Hgo. México

[C] Universidad Autónoma del Estado de Morelos, Centro de Investigaciones Químicas, Av. Universidad 1001, C.P. 62210, Cuernavaca, México.

[D] Centro Universitario de Vinculación de la Benemérita Universidad Autónoma de Puebla, Av. San Claudio, Ciudad Universitaria Col. San Manuel. Puebla, Pue. CP 72570, México.

Received April 17, 2006

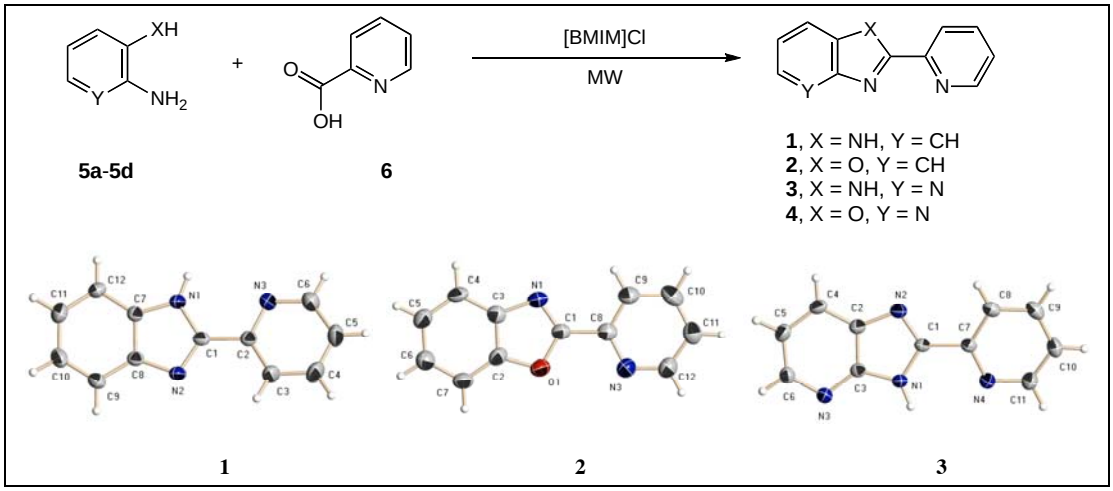

An efficient and fast procedure for the synthesis of 2-(2-pyridyl)azoles is described using ionic liquids as catalysts under microwave irradiation. The X-ray crystallographic analyses for three of the four synthesized compounds are presented. Potentiodynamic polarization studies were carried out to analyze the electrochemical behavior of the compounds in corrosive acidic media. Of the four derivatives, one compound was detected to be an effective corrosion inhibitor prototype for oil refinery environments

J. Heterocyclic Chem., **44**, 145 (2007).

INTRODUCTION

Benzimidazole [1], benzooxazole [2], imidazo[4,5-*b*]pyridine [3] and oxazolo[4,5-*b*]pyridine derivatives [4] are important heterocyclic compounds with well-known biological activity. In addition, these compounds are useful intermediates in organic [5] and polymer synthesis [6], and several pyridine [7], benzimidazole [8] and benzooxazole [9] derivatives have been previously reported as effective corrosion inhibitors.

In recent years, microwave-assisted organic synthesis (MAOS) has attracted considerable interest, due to the generally short reaction times and the circumstance that the resulting products are obtained with high purity and yields [10]. A recent trend in this area is to use ionic liquids (ILs) as solvent, co-solvent and/or catalyst, since they are "ecofriendly" [11] and since their ionic nature allows a very effective coupling with microwave energy [12].

Herein, a successful microwave-promoted synthesis of 2-(2-pyridyl)azoles is reported employing an ionic liquid as catalyst: 2-(2-pyridyl)-1*H*-benzimidazole (**1**), 2-(2-pyridyl)-benzooxazole (**2**), 2-(2-pyridyl)-1*H*-imidazo[4,5-*b*]pyridine (**3**) and 2-(2-pyridyl)oxazole[4,5-*b*]pyridine (**4**). The electrochemical polarization technique was used to test the inhibitory properties of these compounds against SAE 1018 C-steel corrosion in acidic media. Furthermore, the X-ray structures of compounds **1**, **2** and **3** are presented.

RESULTS AND DISCUSSION

Synthesis: Formerly, the most straightforward methods for the preparation of benzoazoles involved the cyclodehydration reaction between *ortho*-substituted aromatic amines and carboxylic acids, which proceeds only under harsh reaction conditions [13].

Similarly, most of the synthetic methods to prepare azole[4,5-*b*]pyridines start from properly substituted pyridines to generate the imidazole or oxazole ring [14], or from conveniently substituted azoles to generate the pyridine ring [15], involving generally more than one reaction step, complicated work-up and modest yields.

Microwave-assisted methodologies have been described for the synthesis of aryl- and 2-methylbenzoazoles, either in the presence [16] or absence of a solvent [17]. Microwave synthesis has also been widely used for the synthesis of many other heterocyclic compounds [18].

Very recently we reported on the microwave-assisted synthesis of 2-long alkyl benzoazoles and azole[4,5-*b*]-pyridines in solvent-free conditions [19], however, this procedure failed when it is applied to the synthesis of 2-pyridyl-substituted analogues, presumably due to the descarboxylation of the picolinic acid (**6**).

After some experimentation we have now discovered that using an ionic liquid as catalyst in the reactions, the descarboxylation of the picolinic acid was inhibited, presumably as a consequence of a C-H···O hydrogen-bonding interaction between the ionic liquid and the oxygen of the hydroxyl group of the picolinic acid. Thus, 2-(2-pyridyl)-benzoazoles (**1** and **2**) and 2-(2-pyridyl)-azole[4,5-*b*]pyridines (**3** and **4**) were prepared very quick and efficiently.

Having evaluated three ionic liquids, ([BMIM]Cl, $[BMIM]BF_4$ and $[BMPy]PF_6$), optimized the microwave reaction conditions such as temperature and power level of irradiation and tested the influence of solvent or solid supports (data not shown), we could establish as optimum parameters for the synthesis of **1**-**4** (Scheme 1), using the conditions shown in Table 1 (catalyst: 1-butyl-3-methyl-imidazolium chloride, [BMIM]Cl).

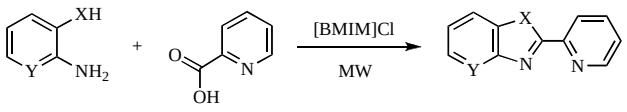

5a-5d **6**

1, X = NH, Y = CH
2, X = O, Y = CH
3, X = NH, Y = N
4, X = O, Y = N

Scheme 1. Synthesis of 2-(2-pyridyl)benzoazoles (**1** and **2**) and 2-(2-pyridyl)azole[4,5-*b*] pyridines (**3** and **4**).

The course of the reactions was followed by thin-layer chromatography using as reference samples prepared by conventional heating (polyphosphoric acid (PPA) as solvent and catalyst, 200°C, 8 h).

Table 1

Reaction conditions and yields for the cyclocondensation reactions of **5** and **6** under solvent-free MW at 600 W (T = 160 ± 5°C) employing [BMIM]Cl, as catalyst.

Compound	Reagent [a]	Time (min) [b]	Yield(%) [c], [d]
(1)	**5a**/**6**	7	84(85)
(2)	**5b**/**6**	8	79(83)
(3)	**5c**/**6**	6	82(80)
(4)	**5d**/**6**	7	80(78)

[a] Molar ratio of reagents **5** and **6**, 1:1.8; [b] Total reaction time of irradiation; [c] Isolated yield; [d] In bracket: isolated yield of the compounds prepared under conventional thermal conditions: 8 hours in PPA at 200°C (see Experimental Section).

Table 2

Crystallographic data for compounds **1**, **2** and **3**.

Crystal data	**1**	**2**	**3**
Formula	$C_{12}H_9N_3$	$C_{12}H\ N_2O$, $4(C_{12}\ H_8\ N_2\ O)$	$C_{11}H_8N_4$
Crystal size (mm)	0.09 x 0.17 x 0.25	0.38 x 0.41 x 0.50	0.39 x 0.42 x 0.45
MW (g mol^{-1})	195.22	981.02	196.21
Space group	Pbca	$P2_1/n$	$P2_1/c$
Cell parameters			
a (Å)	10.7720(17)	6.4390(7)	7.4600(13)
b (Å)	10.1628(16)	21.216(2)	13.497(2)
c (Å)	18.602(3)	17.8046(19)	9.4972(16)
β (°)	90	99.759(2)	102.654(3)
V ($Å^3$)	2036.5(6)	2397.1(4)	933.0(3)
Z	8	2	4
μ (mm^{-1})	0.080	0.090	0.090
ρ_{calcd} (g cm^{-3})	1.273	1.359	1.397
Data collection			
θ limits (°)	$2 < \theta < 27$	$2 < \theta < 25$	$2 < \theta < 26$
No. collected refl.	21252	22836	9504
No. ind. refl. (R_{int})	2226 (0.068)	4230 (0.037)	1832 (0.028)
No. observed refl.[a]	1359	2950	1589
Refinement			
$R^{A,B}$	0.049	0.065	0.036
$R_w^{C,D}$	0.137	0.203	0.095
No. of variables	136	374	139
GOF	1.001	0.970	1.065
$\Delta\rho_{min}$ (e $Å^{-3}$)	-0.19	-0.45	-0.17
$\Delta\rho_{max}$ (e $Å^{-3}$)	0.16	0.52	0.12

[A] $I > 2\sigma(I)$, [B] $R = \Sigma(F_o^2-F_c^2)/\Sigma F_o^2$, [C] all data, [D] $R_w = [\Sigma w(F_o^2-F_c^2)^2/\Sigma w(F_o^2)^2]^{1/2}$

After purification by flash column chromatography, the products were recrystallized from ethanol. In the case of compounds **1**, **2** and **3** the monocrystals obtained permitted the determination of their molecular structures by X-ray crystallography. Although these studies give only information on the molecular structure and intermolecular interactions present in the solid state, these data are helpful for a more profound future understanding of the inhibitory effects present in solution and on metal surfaces (*vide infra*).

X-ray diffraction analysis: The most relevant crystallographic data for compounds **1**, **2** and **3** are shown in Table 2. Selected geometric parameters are summarized in Table 3.

With respect to the molecular structures of compounds **1**-**3** (Figure 2-4) the two heterocyclic rings are almost coplanar between each other (N1-C1-C2-N3 = -13.0° for **1**, O1–C1–C8–N3 = 2.4(4) and 0.3(3)° for **2**, N1–C1–C7–N4 = 13.4(2)° for **3**) and do not present any anomalous features in their planarities, bond distances and aromaticity indices. The bond lengths and bond angles shown in Table 3 agree well with the values observed for related structures [20].

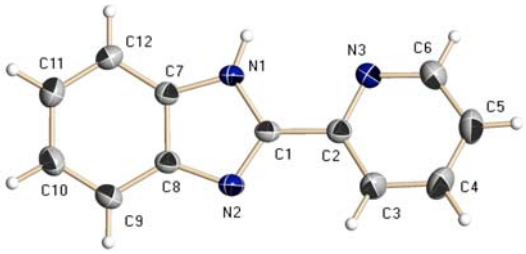

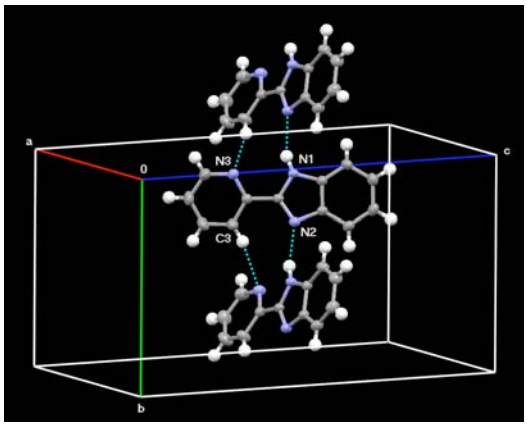

Figure 1. Perspective of the molecular structure of compound **1** and illustration of the most relevant hydrogen-bonding interactions within the crystal lattice.

In all three crystal lattices the 2-(2-pyridyl)benzimidazole and benzoxazole moieties are involved in hydrogen-bonding interactions (Figure 1-3). In the case of the 2-(2-pyridyl)benzimidazole **1** polymeric hydrogen-bonded chains are formed, in which each molecule participates simultaneously in two intermolecular N1-H···N2 (0.860 Å, 2.107 Å, 2.917(2) Å and 156.6º) and C3-H···N3^{i} (0.930 Å, 2.585 Å, 3.487(3) Å, 163.6º; -x+1/2+1,+y+1/2,+z) interactions. Thereby, neighboring molecules are twisted against each other by an angle of 49.9º (Figure 1).

For the 2-(2-pyridyl)benzoxazole **2** there are three independent molecules in the asymmetric unit, each giving an independent polymeric chain with six hydrogen bonds per molecule. Since the hydrogen bonding geometries are very similar for the three chains, for illustrative purposes only the parameters for that described in Figure 2 are indicated: C7-H···N1^{i} (0.930 Å, 2.567 Å, 3.464(4) Å, 162.0º; x+1,+y,+z), C9-H···O1^{ii} (0.930 Å, 2.925 Å, 3.765(4) Å, 150.9º; x-1,+y,+z) and C10-H···N3^{ii} (0.930 Å, 2.940 Å, 3.783(5) Å, 151.4º; x-1,+y,+z).

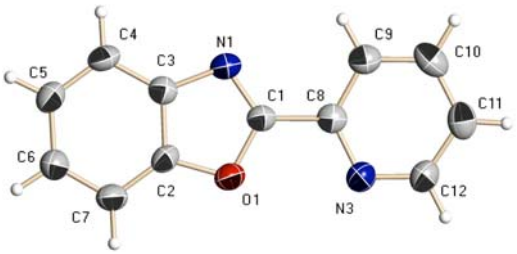

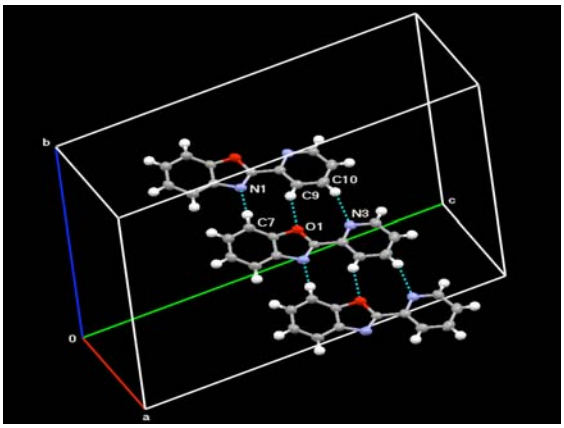

Figure 2. Perspective of the molecular structure of compound **2** and illustration of the most relevant hydrogen-bonding interactions within the crystal lattice.

Comparing the hydrogen bonding interactions between the 2-(2-pyridyl)benzimidazole derivatives **1** and **3**, the pattern changes completely, since the presence of the additional pyridine nitrogen atom in **3** (Figure 3), allows for the formation of a homodimeric motif containing two N-H···N interactions instead of one: N1-H···N3^{i} (0.860 Å, 2.054 Å, 2.889(1) Å and 163.4º; -x+2,-y+1,-z).

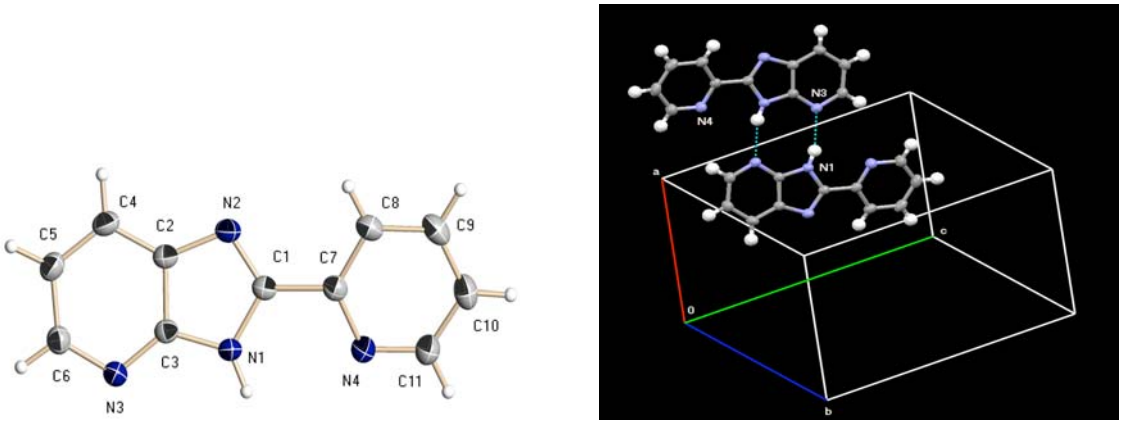

Figure 3. Perspective of the molecular structure of compound **3** and illustration of the most relevant hydrogen-bonding interactions within the crystal lattice.

Table 3

Selected bond lengths, bond angles and torsion angles for compounds **1**, **2** and **3**.

	1	**2**	**3**
***Bond lengths* [Å]**			
C1–N1	1.355(2)	1.285(3) 1.292(3)	1.360(2)
C1–O1	--	1.350(3) 1.359(3)	--
C1–N2	1.317(2)	--	1.314(2)
***Bond angles* [°]**			
N1–C1–N2	113.07(16)	--	113.7(1)
O1–C1–N1	--	115.5(3) 115.2(2)	--
***Torsion angles* [°]**			
N1–C1–C2–N3	-13.0(3)	--	--
O1–C1–C8–N3	--	2.4(4) 0.3(3)	--
N1–C1–C7–N4	--	--	13.4(2)

Potentiodynamic polarization: The potentiodynamic polarization method was used to determine the inhibition properties of the synthesized compounds. To carry out the test a typical three-electrode cell was used, in which the working electrode interacts with the corrosive media, without and with each compound, during different immersion times (10 min, 3 h, 24 h). The corrosive environment employed in this study is one of the most severe used to evaluate metals and alloys submitted to corrosion stress or hydrogen induced cracking.

Figure 4 shows the electrochemical response for the system without additives during different immersion times. This figure indicates that after three hours of exposition, the anodic and cathodic currents diminished, when compared to the system that was immersed only for 10 minutes, probably due to the presence of a film of corrosion products. However, after 24 hours of exposition time, both currents have increased again, indicating that the film has dissolved, such as it has been reported in the literature [21].

The modifications of the currents shown by the systems in function of the immersion time indicate that the corrosion behavior changes over the time and, at present, these results provide an efficient way to compare the system responses with the effects of inhibitors on it.

In order to determine the concentration, at which the best inhibitory effect of each compound could be observed, a polarization study was carried out. Several concentrations of each compound were tested. Figure 5 shows only the polarization curves for compound **1**, since these are representative for all four compound responses. It can be observed that the cathodic process is very sensitive to the variation of the concentration, while the anodic process shows only slight changes.

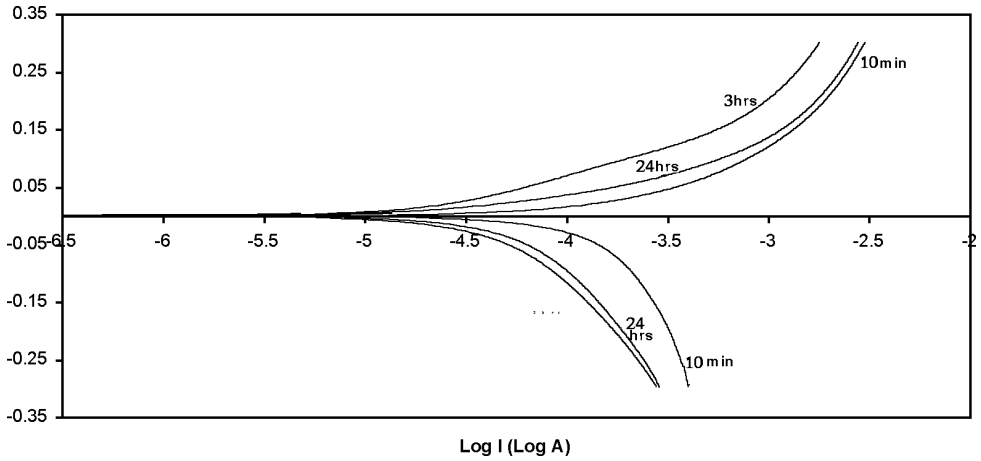

Figure 4. Polarization curves obtained on the system SAE 1018 carbon steel in acidic media for different immersion times (10 min, 3 h, 24 h). Scan speed 0.1 mV/seg.

On the other hand, the sample with a concentration of 100 ppm presents a visible change in comparison to the system without additives. Since this concentration is considered the maximum usable, in most of the laboratory studies, it was decided to use this concentration to test the immersion time effect on the systems with each of the synthesized compounds.

For this purpose, each compound was added to the system and left to act on the steel electrode surface during 10 minutes (time 0), 3 and 24 hours. The results showed that every compound has a main effect on the cathodic the currents. On the other hand, the variations of the oxidation currents were small.

In order to analyze the results quantitatively, the corrosion parameters were calculated from the polarization curves. Corrosion potential, polarization resistance and corrosion current are shown in Table 4.

The corrosion potentials of the systems containing 100 ppm of the corresponding compound display very little variation with respect to the additive-free system, so that the surface energetic conditions are not greatly affected by the presence of the compounds. On the other hand, the

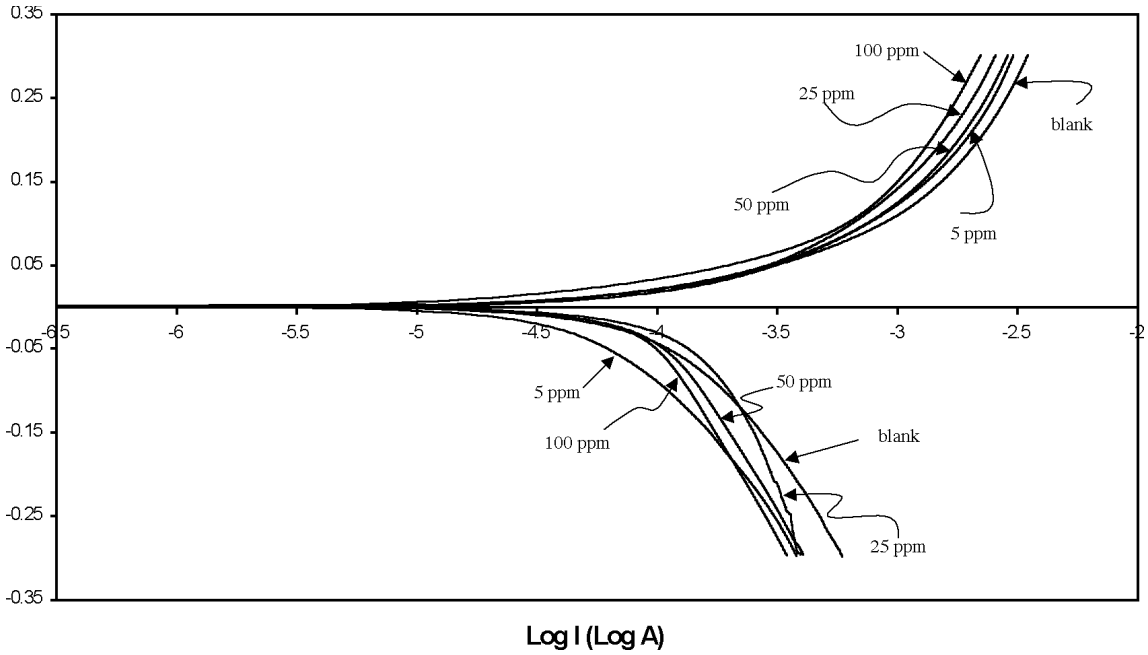

Figure 5. Polarization curves obtained on the system SAE 1018 carbon steel in acidic media for different concentrations of compound **1** after 24 hours of inmertion time. Scan speed 0.1 mV/seg.

process: the longer the immersion time, the lower were

Table 4

Corrosion parameters obtained from the polarization curves for the SAE 1018 carbon steel system immersed in an acidic environment of the type NACE 0177.

Compound	Immersion time(h)	E_{corr} (V)	*Rp* (ohm)	I_{corr} (A)
blank	0	-0.616	209.12	9.56×10^{-5}
	3	-0.638	865.41	2.30×10^{-5}
	24	-0.630	484.72	4.10×10^{-5}
1	0	-0.616	485.93	4.12×10^{-5}
	3	-0.609	641.37	3.12×10^{-5}
	24	-0.614	1282.1	1.56×10^{-5}
2	0	-0.618	146.66	1.36×10^{-4}
	3	-0.627	505.2	3.96×10^{-5}
	24	-0.644	761.25	2.63×10^{-5}
3	0	-0.636	132.95	1.50×10^{-4}
	3	-0.637	546.37	3.66×10^{-5}
	24	-0.666	784.59	2.55×10^{-5}
4	0	-0.625	166.04	1.20×10^{-4}
	3	-0.623	482.15	4.15×10^{-5}
	24	-0.645	856.48	2.34×10^{-5}

polarization resistance is more sensitive and a quantitative comparison can be made.

The corrosion currents were calculated from the polarization curves and the polarization resistances obtained in the range of $E_{corr} \pm 0.02$ V. This analysis showed that the corrosion currents were always higher than that of the additive-free system, with exception of compound **1**, and after 3 hours all values were higher than that of the blank.

These results also indicate that the evaluated compounds present a type of competence with corrosive agents such that the double layer could be modified because of the strong interaction between the compounds and the metallic surface.

After 24 hours of immersion time, a significant decrease of the corrosion currents was observed, being compound **1** that, which presented the lowest corrosion current (see Table 4). This fact indicates that compound **1** could be an effective corrosion inhibitor prototype (efficiency: 86% at 100 ppm) in oil refinery environments.

All compounds presented a very thin film on the electrode surface that was, visible with an optical microscope, but this film was homogeneous and without fissures only for compound **1**.

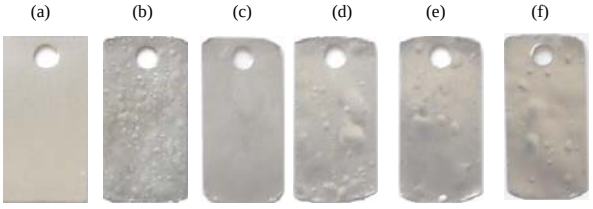

Figure 6. Micrographs of blistering formed on the 1018 carbon steel surface in acidic corrosive solution at pH 4.0 after 48 hours of exposure at 60°C: (a) testing coupon, (b) without additives, (c) 50 ppm of **1**, (d) 50 ppm of **2**, (e) 50 ppm of **3** and (f) 50 ppm of **4**.

Figure 6 shows the micrographs of the carbon steel specimens exposed during 48 hours the corrosive environment used in this study, with and without the addition of 50 ppm of compounds **1**-**4**. The protective effect of the compounds **1** is clearly observed.

An explanation for the electrochemical behavior and the inhibitory effects of these compounds is not straightforward, since there are several possibilities for the metal-inhibitor interaction, considering that the atoms at the metal surface may be neutral or oxidized: (i) the formation of coordinative bonds with the donating atoms of the ligand, (ii) the occurrence of an interaction with the π–electron density of the ligands and (iii) the presence of hydrogen-bonding and other electrostatic interactions, considering that some of the metal centers at the metal surface may carry already substituents such as oxygen or sulfur form the corrosive medium. According to the crystallographic data and theoretical studies we have carried out on the present ligands [22], each of the three inhibition mechanisms is feasible for the compounds studied herein. The molecules are planar or almost planar (extensive π–electron density), positively charged in the corrosive medium (protonated form) and capable of strong hydrogen-bonding interactions. The theoretical calculations above have shown that there is a correlation between the hardness of the compounds tested as inhibitors and the inhibitory efficiency, assuming that the adsorption to the metal surface results from an interactions with the π–electrons (including backdonation) [23].

CONCLUSIONS

A new microwave-assisted methodology, using an ionic liquid as catalyst, was developed that is quick and efficient to synthesize 2-pyridyl-azoles. The compounds synthesized present a potentiodynamic behavior that

indicates the formation of a thin film, most probably consisting also of corrosion products, that protects the metallic surface from an acidic corrosive environment. The inhibitory behavior was markedly enhanced for the system containing 2-(2-pyridyl)-1*H*-benzimidazole as inhibitor.

EXPERIMENTAL

Materials. All reagents (Aldrich) were used without previous purification except 1-methylimidazole (99%) and pyridine (99%), which were vacuum-distilled from CaH_2 prior to use. 1-Butyl-3-methylimidazolium chloride ([BMIM]Cl) and 1-Butyl-3-methylimidazolium tetrafluoro borate ([BMIM]PF_6) were synthesized by a literature procedure **[24]**.

Measurements. Melting points are not corrected and were measured in a Fisher Scientific apparatus with a 300°C thermometer. FT-IR spectra were registered on a Nicolet FT-IR 5DX FT spectrometer as KBr discs. Specific rotation was measured in a Perkin Elmer 241 polarimeter. ^{1}H NMR (300 MHz) and ^{13}C NMR (75.4 MHz) spectra were obtained with Jeol Eclipse-300 equipment using TMS as internal standard. Mass spectra were recorded on HP 5973 equipment with a selective mass detector. Elemental analyses were obtained on a CHNO/S Perkin-Elmer analyzer.

Microwave irradiations were carried out utilizing a controlled single-mode MW equipment (MIC-I, 2450 MHz, power max. 600 W, from SEV, Mexico) [25]. Open reaction tubes (diameter: 5 cm, capacity 50 mL) were used, and temperature was measured by an on-line IR detector.

General Procedure for the Synthesis of compounds 1-4 by Thermal Procedure. The corresponding amine (**5**) (1.0 mmol) and picolinic acid (**6**) (0.22 g, 1.8 mmol) were mixed with a sufficient quantity of polyphosphoric acid (PPA) to give a stirrable paste. The mixture was heated slowly to 180-200°C and kept at this temperature for 8 h. The reaction mixture was slowly cooled to 100°C and added into a large volume of water. The insoluble residue was collected by filtration, washed with a solution containing 10% sodium carbonate and then with water. The crude product was dried at 60°C and recrystallized twice from an aqueous alcohol mixture subsequent to treatment with a small amount of activated charcoal.

General Procedure for the Synthesis of Compounds 1-4 under Microwave Irradiation. The corresponding amine (**5**) (1.0 mmol), picolinic acid (**6**) (0.22 g, 1.8 mmol) and 0.1 g of [BMIM]Cl were charged into a large open vial. The vial was irradiated at 600 W (T = 160 ± 5°C) under stirring during the time indicated in Table 1. Each 30 seconds the irradiation was stopped during 5 seconds to avoid overheating. After cooling, the crude products were purified through silica-gel chromatography column using the eluent specified en each case and then recrystallized from ethanol.

2-(2-Pyridyl)-1*H*-benzimidazole (1). This compounds was obtained as colorless crystalline solid, 84% yield, eluent: acetone/hexane gradient, mp 218-220°C (lit. [13f] 218°C); ir (potassium bromide): 3429, 3056, 2959, 1600, 1449, 1398, 1317, 1285, 998, 746, 699 cm^{-1}; ^{1}H nmr (DMSO-d_6): δ 8.70 (dt, J = 4.8, 0.8 Hz, 1H), 8.34 (dt, J = 8.0, 1.0 Hz, 1H), 7.98 (td, J = 8.0, 1.6 Hz, 1H), 7.68-7.60 (m, 2H), 7.49 (ddd, J = 4.6, 3.0, 1,4, 1.0 Hz, 1H), 7.29-7.18 (m, 2H) ppm; ^{13}C nmr (DMSO-d_6): 116.3, 119.2, 122.1, 123.2, 124.2, 125.4, 135.0, 138.2, 143.9, 149.2, 150.1, 151.4 ppm.

2-(2-Pyridyl)-1*H*-benzooxazole (2). Colorless crystalline solid, 79% yield, eluent acetone/hexane gradient, mp 108-109°C (lit. [14a] 108°C); ir (potassium bromide): 3425, 3060, 2986, 1588, 1553, 1456, 1243, 1076, 738 cm^{-1}. ^{1}H nmr (DMSO-d_6): 8.75 (dt, J = 4.8, 0.8 Hz, 1H), 8.28 (dt, J = 8.0, 1.0 Hz, 1H), 8.00 (td, J = 8.0, 1.6 Hz, 1H), 7.84-7.77 (m, 2H), 7.58 (ddd, J = 4.6, 3.0, 1.4, 1.0 Hz, 1H), 7.47-7.35 (m, 2H) ppm; ^{13}C nmr (DMSO-d_6): 111.3, 120.3, 123.5, 125.1, 126.2, 137.61, 141.2, 145.2, 150.2, 150.4, 161.3 ppm.

2-(2-Pyridyl)-1*H*-imidazole[4,5-*b*]pyridine (3). Colorless crystalline solid; yield: 82%, eluent: acetone/ethyl acetate gradient; mp 226-228°C; ir (potassium bromide): 3441, 3049, 2963, 1588, 1449, 1270, 1115, 773, 699 cm^{-1}, ^{1}H nmr (DMSO-d_6): 8.75 (dt, J = 4.8, 0.8 Hz, 1H), 8.39-8.34 (m, 2H), 8.06-7.88 (m, 2H), 7.56 (ddd, J = 4.6, 3.0, 1.4, 1.0 Hz, 1H), 7.26 (dd, J = 4.6, 3.4 Hz, 1H) ppm; ^{13}C nmr (DMSO-d_6): 118.6, 120.0, 122.1, 125.2, 135.6, 137.6, 145.5, 148.0, 150.0, 152.3, 156.5 ppm. *Anal.* Cacld. for $C_{11}H_8N_4$: C 67.34, H, 4.11, N 28.55. Found: C 66.98, H 4.13, N 28.40.

2-(2-Pyridyl)-1*H*-oxazole[4,5-*b*]pyridine (4). Colorless crystalline solid, 80% yield, eluent: acetone, mp 182-184°C (lit. [4d] 197-198°C); ir (potassium bromide): 3421, 3068, 2990, 1584, 1557, 1464, 1406, 1258, 1072, 784, 695 cm^{-1}. ^{1}H NMR (DMSO-d_6): 8.81 (dt, J_1 = 4.8 Hz, J_2 = 0.8 Hz, 1H), 8.59 (dd, J_1 = 4.6 Hz, J_2 = 1.4 Hz, 1H), 8.38 (dt, J_1 = 8.0 Hz, J_2 = 1.0 Hz, 1H), 8.29 (dd, J_1 = 8.0 Hz, J_2 = 1.0 Hz, 1H); 8.08 (td, J_1 = 1.6 Hz, J_2 = 8.0 Hz, 1H), 7.66 (ddd, J_1 = 1.0 Hz, J_2 = 1.4 Hz, J_3 = 3.0 Hz, J_4 = 4.6 Hz, 1H), 7.50 (dd, J_1 = 4.8 Hz, J_2 = 3.6 Hz, 1H) ppm; ^{13}C nmr (DMSO-d_6): 120.4, 122.1, 125.0, 127.6, 138.5, 143.8, 145.4, 147.7, 151.0, 155.8, 164.3 ppm.

X-ray Crystallgraphy. X-ray diffraction data were collected on a Bruker-AXS diffractometer with a CCD area detector ($\lambda_{MoK\alpha}$= 0.71073 Å, monochromator: graphite). Frames were collected at T = 293 K via ω/Φ–rotation at 10 s per frame [26]. The measured intensities were reduced to F^2 and corrected for absorption with SADABS [27]. Corrections were made for Lorentz and polarization effects. Structure solution, refinement and data output were carried out with the SHELXTL-NT program package [28]. Non hydrogen atoms were refined anisotropically. C-H hydrogen atoms were placed in geometrically calculated positions using a riding model. N-H hydrogen atoms have been localized by difference Fourier maps and refined fixing the bond length to 0.86 Å; that isotropic temperature factors have been fixed to a value 1.5 times the one of the oxygen atoms. Figures were created with SHELXTL-NT and MERCURY [29]. Hydrogen bonding interactions in the crystal lattice were calculated by PLATON [30].

One of the three independent molecules in the crystal lattice of compound **2** is disordered over two positions, and as a consequence restraints had to be applied in order to obtain a reasonable structure. Therefore, the corresponding hydrogen atoms have not been calculated and the R values are higher than for the other compounds.

Crystallographic data for the structures reported in this paper have been deposited with the Cambridge Crystallographic Data Centre as supplementary publications no. CCDC-292606-292608. Copies of the data can be obtained free of charge on application to CCDC, 12 Union Road, Cambridge CB2 1EZ, UK (fax: (+44)1223-336-033; e-mail: deposit@ccdc.cam.ac.uk, www: http://www.ccdc.cam.ac.uk).

Potentiodynamic Polarization. Potentiodynamic polarization tests were carried out using a typical three-electrode cell within the range of E_{corr} ± 0.3 V. A calomel electrode was used as reference, graphite bar as a counter electrode and a carbon steel (SAE 1018) disc with 0.503 cm^2 transversal area as working electrode. This electrode was polished before each test with SIC emery paper (600 grid) and rinsed with deionized water.

Corrosive Solution Preparation. A corrosive environment of the type used in the NACE TM 0177 method was prepared. The composition of the solution used was: 0.04 M CH_3COOH/ $NaOOCCH_3$, pH = 3.5; 30 172 ppm Cl^- as NaCl (0.52 M Chloride). The solution was prepared with deionized water, deaerated with gaseous nitrogen. Analytical grade reagents were employed.

Preparation of the Inhibitor Solutions (with 1-4). For each inhibitor, a 10,000 ppm solution was prepared from 1.00 g of the compound, which was dissolved in DMSO (10 mL). Depending on the inhibitor concentration required, a proportional volume of the compound was calculated, and deposited in a 100 mL volumetric flask that was filled up with the corrosive solution.

Testing Preparation. The testing consisted of carbon steel 1018 specimens (2.54 x 1.25 x 0.025). Sheet specimens were ground with silica sand retained in a mesh number 100 in a universal mixer ERWEKA model AR 400 at 100 rpm for 72 h. To remove the corrosion products formed on the metallic surface after grounding, samples were ultrasonically degreased in hexane, rinsed in double distilled water and acetone, dried in a forced current of nitrogen and kept in a desiccator before being exposed to the aqueous test environment.

Experiment for the Specimens Corrosion. The specimens were immersed into the glass cells containing 100 mL of the corrosive solution and 0 (blank) and 50 ppm of **1**-**4**, respectively. Experiments were performed at 60 ºC for 48 h. The cells were placed in a rotator dynamic evaluator model C5-EDP-020-D. After of the exposure time, the specimen was taken out and washed with double distilled water. The corrosion product on the steel surface was mechanically removed by rubbing it with a brush. The specimens were washed in an ultrasonic bath with acetone, dried in a flux of high purity nitrogen, set to dry in a stove at 100 ºC by 2 h.

Surface Examination. Blistering surfaces were observed and recording by using a velocity high camera model Kodak Mega Plus ES310/T; controlled by a PC through the IMAQ Vision Builder software provided by National Instruments.

REFERENCES

[1a] W. A. Denny, G. W. Rewcastle and B. Baguley, *J. Med. Chem.*, **33**, 814 (1990); [b] C. Cermelli, G. Baggio, L. Lupo, M. Malagoli, M. Castelli, L. Garuti, L and Varoli, L, *Anti-cancer Drug Design*, **13**, 969 (1998); [c] M. L. López-Rodríguez, B. Benhamú, A. Viso, M. J. Morcillo, M. Murcia, L. Orensanz, M. J. Alfaro and M. I. Martín, *Bioorg. Med. Chem.*, **7**, 2271 (1999); [d] H. Akamatzu, K. Fukase and S. Kusumoto, *J. Comb. Chem.*, **4**, 475 (2002); [e] K. Kopan´ska, K., A. Najda, J. Z&dotebrowska, L. Chomicz, J. Piekarczyk, P. Myjak and M. Bretner, *Biorg. Med. Chem.*, **12**, 2617 (2004).

[2a] J. V. Hernández, A. I. Oliva, L. Simón, F. M. Muñiz, A. A. Mateos and J. R. Moran, *J. Org. Chem.,* **68**, 7513 (2003); [b] S. Ünlü, S. Nacak Baytas, E. Kupeli and E. Yesilada, *Archiv Pharmazie*, **336**, 310 (2003); [c] I. Yildiz-Oren, B. Tekiner-Gulbas, I. Yalcin, O. Temiz-Arpaci, E. Ak-Sener, N. Altanlar, *Archiv Pharmazie,* **337**, 402 (2004).

[3a] G. Cristalli, S. Vittori, A. Eleuteri, R. Volpini, E. Camaioni, G. Lupidi, N. Mohmoud, F. Bevilacqua and G. J. Palu, *J. Med. Chem.*, **38**, 4019 (1995); [b] D. J. Cundy, G. Holan, M. Otaegui and G. W. Simpson, *Bioorg. Med. Chem. Lett.*, **7**, 669 (1997); [c] A. G. Arvanitis, J. T. Rescinito, C. R. Arnold, R. G. Wilde, G. A. Cain, J. H. Sun, J.-S. Yan, C. A. Teleha, L. W. Fitzgerald, J. McElroy, R. Zaczek, P. R. Hartig, S. Grossman, S. P. Arneric, P. J. Gilligan, R. E. Olson and D. W. Roberston, *Biorg. Med. Chem. Lett.*, **13**, 125 (2003).

[4a] V. Grumel, J.-Y. Mérour and G. Guillaumet, *Heterocycles,* **55**, 1329 (2001); [b] C. W. Phoon, P. Y. Ng, A. E. Ting, S. L. Yeo and M. M. Sim, *Bioorg. Med. Chem. Lett.*, **11**, 1647 (2001); [c] A. Pinar, P. Yurdakul, I. Yildiz, O. Temiz-Arpaci, N. L. Acan, E. Aki-Sener and I. Yalcin, *Biochem. Biophys. Res. Commun.*, **317**, 670 (2004).

[5a] M. R. Grimmett, in Comprehensive Heterocyclic Chemistry, ed, Pergamon, New York, NY, 1984, pp. 345-498; [b] G. V. Boyd, in Comprehensive Heterocyclic Chemistry, ed, Pergamon, New York, NY, 1984, pp. 177-233; [c] A.-B. A. M. Ghattas and H. M. Moustafa, *Synth. Commun.*, **30**, 3423 (2000); [d] M. Gupta, P. Mathur and R. J. Butcher, *Inorg. Chem.,* **40**, 878 (2001).

[6a] M. Berrada, Z. Anbaoui, N. Lajrhed, M. Berrada and N. Knouzi, *Chem. Mat.*, **9**, 1989 (1999); [b] M. Berrada, F. Carriere, A. Abourriche, A. Benamara, N. Lajrhed, M. Kabbaj and M. Berrada, *Mat. Chem.*, **12**, 3551 (2002); [c] H. H. Wang and S. P. Wu, *J. Appl. Polym. Sci.,* **90**, 1435 (2003); [d] L.-C. S. Hsu, K. Ch. Chang, Y. P. Huang and S. J. Tsai, *J. Appl. Polym. Sci.,* **88**, 2388 (2003).

[7a] M. Kliskic, J. Radisevic and S. Gudic, J. *Appl. Electrochem.*, **27**, 947 (1997); [b] V. S. Sastri and J. R. Perumaredi, *Corrosion*, **50**, 432 (1994); [c] V. S. Sastri and J. R. Perumareddi, *Corrosion*, **53**, 617 (1997); [d] Y. Xiao-Ci, Z. Hong, L. Ming-Dao, R. Hong-Xuan and Y. Lu-An, *Corrosion Sci.*, **42**, 645 (2000); [e] M. Lashgari, M. R. Arshadi and Gh. A. Parsafar, *Corrosion,* **61**, 780 (2005); [f] M. A. Veloz and I. González, *Corrosion*, **62**, 283 (2006).

[8a] G. Lewis, *Corrosion Sci.*, **22**, 579 (1982); [b] A. Popova, M. Christov and T. Deligeorgiev, *Corrosion*, **59**, 756 (2003); [c] M. Christov and A. Popova, *Corrosion Sci.*, **46**, 1613 (2004); [d] A. Popova, M. Christov and T. Deligeorgiev, *Corrosion Sci.*, **46**, 1333 (2004).

[9a] A. M. Al-Mayouf, A. A. Al-Suhybani and A. K. Al-Ameery, *Desalination,* **116**, 25 (1998); [b] D.-q. Zhang, L.-x. Gao and G.-d. Zhou, *Corrosion Sci.*, **46**, 3031 (2004).

[10a] A. Loupy, Microwave in Organic Synthesis, Wiley-VCH, Weinheim, 2002; [b] B. L. Hayes, Microwave Synthesis: Chemistry at the Speed of Light, CEM Publishing, Matthews, 2002; [c] P. Lidström and J. P. Tierney, Microwave-Assisted Organic Synthesis, Blackwell Scientific, 2005; [d] C. O. Kappe, Microwaves in Organic and Medicinal Chemistry, Wiley-VCH, Weinheim, 2005; [e] R. Martínez-Palou, Química en Microondas, CEM Publishing, Matthews, 2006.

[11a] T. Welton, *Chem. Rev.*, **99**, 2071 (1999); [b] H. Zhao and S. V. Malhotra, *Aldrichimica Acta*, **35**, 75 (2002); [c] S. A. Forsyth, J. M. Pringle and D. R. MacFarlane, *Aust. J. Chem.*, **57**, 113 (2004); [d] P. J. Scammells, J. A. Scott and R. D. Singer, *Aust. J. Chem.*, **158**, 155 (2005); [e] P. Wasserscheid and W. Keim, Ionic Liquids in Synthesis, Wiley-VCH, Wenheim, 2004.

[12a] N. E. Leadbeater, H. M. Torenius H. Tye, *Comb. Chem. High Throughput Screen.*, **7**, 511 (2004); [b] K. G. Mayo, G. H. Nearhoof and J. J. Kiddle, *Org. Lett.*, **4**, 1567 (2002); [c] S. Garbacia, B. Desai, O. Lavastre and C. O. Kappe, *J. Org. Chem.* **68**, 9136 (2003); [d] N. Srinivaasan and A. Ganesan, *Chem. Commun.* 916 (2003); [e] Y. Peng and G. Song, *Tetrahedron Lett.* **45**, 5313 (2004); [f] Y.-H. Yen and Y.-H, Chu, *Tetrahedron Lett.* **45**, 8137 (2004); [g] K. M. Brummond and D. Chen, *Org. Lett.* **7**, 3473 (2005).

[13a] D. H. Hein and R. J. Halmeim, *J. Am. Chem. Soc.*, **79**, 427 (1957); [b] J. M. Aizpurua and C. Palomo, *Bull. Soc. Chim. Fr.*, **II**, 142 (1984); [c] P. Savarino, R. Carpignano, G. Viscardi E. Barni and G. Di Modica, *J. Heterocyclic Chem.*, **25**, 1675 (1988); [d] A. O. Aldehamid, C. Párkanyi, S. M. K. Rashid and W. D. Lloyd, *J. Heterocyclic Chem.*, **25**, 403 (1988); [e] E. Alcalde, L. Pérez-García, I. Dinarés and J. Frigola, *J. Org. Chem.*, **56**, 6516 (1991); [f] A. B. Alloum, K. Bougrin and M. Soufiaoui, *Tetrahedron Lett.*, **44**, 5935 (2003).

[14a] V. I. Cohen, *J. Heterocyclic Chem.*, **16**, 13 (1979); [b] A. D. Redhouse, R. J. Thompson, B. J. Wakefield and J. A. Wardell,

Tetrahedron, **48**, 7619 (1992); [c] I. K. Khanna, R. M. Weier, K. T. Lentz, L. Swenton and D. C. Lankin, *J. Org. Chem.*, **60**, 960 (1995); [d] E. Garnier, S. Blanchard, I. Rodríguez, C. Jary, J.-M. Léger and P. Caubére, *Synlett*, 2033 (2003).

[15a] J. E. Francis and M. A. Moskal, *Can. J. Chem.*, **70**, 1288 (1992); [b] M. Y. Chu-Moyer and R. Berger, *J. Org. Chem.*, **60**, 5721 (1995); [c] F. Perandones and J. L. Soto, *J. Heterocycl. Chem.*, **34**, 107 (1997); [d] M. E. Zaki, M. E., F. Poenca and B. L. Booth, *J. Org. Chem.*, **68**, 276 (2003).

[16a] A. C. S. Reedy, P. S. Rao and R. V. Venkataraman, *Tetrahedron*, **53**, 5847 (1997); [b] P. M. Bendale and C.-M. Sun, *J. Comb. Chem.*, **4**, 359 (2002); [c] H. Yu, H. Kawanishi and H. Koshima, *Heterocycles*, **60**, 1457 (2003); [d] R. S. Pottorf, N. K. Chadha, M. Katkevics, V. Ozola, E. Suna, H. Ghane, T. Regberg and M. R. Player, *Tetrahedron Lett.*, **44**, 175 (2003).

[17a] K. Bougrin and M. Soufiaoui, *Tetrahedron Lett.*, **36**, 3683 (1995); [b] D. Villemin, M. Hammadi and B. Martin, *Synth. Commun.*, **26**, 2895 (1996); [c] K. Bougrin, A. Loupy and M. Soufiaoui, *Tetrahedron Lett.*, **54**, 8055 (1998); [d] A. B. Alloum, S. Bakkas and M. Soufiaoui, *Tetrahedron Lett.*, **39**, 4481 (1998); [e] K. Bougrin, A. Loupy, A. Petit, B. Daou and M. Soufiaoui, *Tetrahedron*, **57**, 163 (2001); [f] Y. Njoya, N. Boufatah, A. Gellis, P. Rathelot, M. P. Crozet and P. Vanelle, *Heterocycles*, **57**, 1423 (2002).

[18a] Y. Xu and Q.-X. Guo, *Heterocycles* **63**, 903 (2004). [b] A. R. Katritzky and S. K. Singh, *ARKIVOC* **xiii**, 68 (2003).

[19] R. Martínez-Palou, L. G. Zepeda, H. Höpfl, A. Montoya, D. J. Guzmán-Lucero and J. Guzmán, *Mol. Diversity*, **9**, 631 (2005).

[20] Cambridge Structural Database, Cambridge Crystallographic Data Centre, version 5.26, November **2004**, Cambridge, UK.

[21] M. A. Veloz and I. González, *Electrochim. Acta*, **48**, 135 (2002).

[22] V. S. Sastri, M. Elboujdani and J. R. Perumareddi, *Corrosion*, **61**, 933 (2005).

[23] B. Gómez, N. V. Likhanova, M. A. Domínguez-Aguilar, R. Martínez-Palou, A. Vela and J- L. Gázquez, *J. Phys. Chem. B*, **110**, 8928 (2006).

[24] N. E. Leadbeater and H. M. Torenius, *Tetrahedron*, **59**, 2253 (2003).

[25] Web page: **www.sevmexico.com**

[26] Bruker Analytical X-ray Systems. *SMART*: Bruker Molecular Analysis Research Tool, Version 5.618, **2000**.

[27] Bruker Analytical X-ray Systems. *SAINT + NT*, version 6.04, **2001**.

[28] G. M. Sheldrick, *SHELX86* **1986** (University of Göttingen: Göttingen), **1986**; Bruker Analytical X ray Systems. *SHELXTL-NT* version 6.10, **2000**.

[29] *MERCURY*, version 1.4, Cambridge Crystallographic Data Centre, Cambridge, **2005**.

[30] *PLATON*, version 210103, Spek, A. L. *Acta Cryst.* **1990**, *A46*, C-34.